

# FINAL STATE INTERACTIONS IN NEUTRINO–NUCLEUS EXPERIMENTS\*

STEVEN DYTMAN

University of Pittsburgh, Physics and Astronomy Department  
100 Allen Hall, 3941 O'Hara Street, Pittsburgh, PA 15260, USA

*(Received July 15, 2009)*

Many neutrino–nucleus experiments need to find quasifree events in order to measure the beam energy which is an important part of oscillation measurements. Final state interactions are very important because they can mask the topology of an event. This paper reviews some of the concepts important in a good final state model and provides some detail for what is used in GENIE.

PACS numbers: 13.15.+g, 14.60.Pq

## 1. Introduction

Monte Carlo codes are important to simulations of neutrino experiments. Low event rates force use of large monolithic detectors with materials such as carbon, water, or iron. Monte Carlo (MC) simulations, the focus of the Ładdek winter school are key to understanding experiments. Final state interactions (FSI) are an important component of every MC because we all desire to see evidence of the primary vertex in each event. FSI provide an important way to mask the identity of the primary vertex. The goal of this paper is to provide a short guide to strong interactions. Since the author built the GENIE FSI codes, it will provide the main examples.

Neutrinos are different than any other particle in various ways. While neutrinos have a mean free path (MFP) of a “light year in lead”, hadrons typically interact within a few cm of normal material. When produced inside a nucleus, hadrons have a typical MFP of a few femtometers. Detectors in a neutrino experiment are almost always composed of nuclei today. Therefore, the hadrons produced in the primary interaction (what the neutrino does directly) often (*e.g.*  $\sim 30\%$  in iron for few GeV neutrinos) have

---

\* Presented at the 45th Winter School in Theoretical Physics “Neutrino Interactions: From Theory to Monte Carlo Simulations”, Ładdek-Zdrój, Poland, February 2–11, 2009.

a FSI. There are many possibilities from benign to dangerous. For example, a quasielastic (QE) interaction that emits a proton can end up with a final state of 3 protons, 2 neutrons, and a few photons with finite probability. For a 1 GeV muon neutrino QE interaction in carbon, the probability of a final state different than 1 proton is 35% (GENIE). A possibility even worse is a pion production primary interaction where the pion is absorbed. Such an event occurs for 20% (GENIE) of pion production events and can look like a QE event. At minimum, the wrong beam energy will be measured for these events as the topology is often mistaken. A high quality Monte Carlo code is the only way to understand the role of these events. Figure 1 shows the pion energies that are relevant to a  $\nu_\mu C$  experiment at 1 GeV; we must understand the interactions of pions of up to about 0.8 GeV kinetic energy. From the left figure, we see that the  $\Delta$  resonance dominates the response for pion production, but provides only about half of all pions. The right figure shows that the spectrum of pions is significantly altered by FSI.

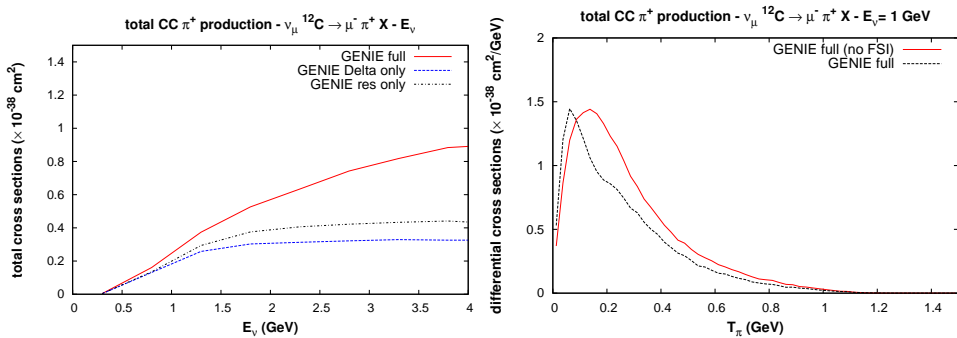


Fig. 1. Left:  $\pi^+$  total cross-section resulting from  $\nu_\mu^{12}\text{C}$  interactions. Different lines show results including all sources, all resonances, and the  $\Delta$  resonance alone. The nonresonant processes are significant in GENIE. Right: Comparison of the  $\pi^+$  momentum distribution due to the bare resonance interaction and what is seen in the final state.

The best way to understand the effects of FSI is to measure the *cross-sections* for as many final states as possible with neutrino beams. At this time, the storehouse for this kind of data is very bare. Dedicated cross-section experiments such as SciBooNE and MINER $\nu$ A will bridge this gap, but we will always be dependent on hadron–nucleus and photon–nucleus experiments for some information. These experiments measure very useful properties of hadrons propagating in nuclei. Although hadron beams are always composed free particles, neutrino experiments need the properties of hadrons produced off-shell in the nucleus. (Pion photoproduction exper-

iments provide useful bridge reactions. Pion FSI are always an important part of all theory calculations for these experiments; the models always come from pion–nucleus data.) The correct attitude is to validate FSI models for neutrino–nucleus with hadron–nucleus data, then use these models to make first predictions of the upcoming dedicated cross-section experiments.

Various models are available. Quantum mechanical models for hadron–nucleus experiments would be the most correct, but difficulties in tracking multiple particles make such a calculation impossible. Semi-classical models have some success in describing pion–nucleus interaction data and are now being applied to neutrino interactions [6]. However, intranuclear cascade (INC) models [10, 11] provided the most important means to understand pion–nucleus data where the final state was highly inelastic, *i.e.* the kinds of data most important for neutrinos. In the semi-classical or INC models, the hadron sees a nucleus of (largely) isolated nucleons (neutrons and protons). The probability of interaction is governed by the *free* cross-section and the density of nucleons,

$$\lambda(E, r) = \frac{1}{\sigma_{hN, \text{tot}} \rho(r)} . \quad (1)$$

The actual class of interaction is then chosen according to the cross-sections for various reactions for free nucleons, sometimes modified for nuclear medium effects.

## 2. Models

Semi-classical models have advanced significantly due to the work of the Giessen group [6] in building a new program called GiBUU. The strong interaction section [7] is the most complete part of the package. The dominant interaction of pions is through resonance formation and they are handled with care. Nucleons in the nucleus are corrected for binding with a local potential well and for Fermi motion with a local Fermi momentum. Resonance production is corrected for the nearby nucleons in a local density approximation. Nonresonant reactions are added by hand. Allowing for the nonlocality of the interaction is an important recent advance. The classical part of the model comes from the use of free cross-sections with corrections rather than quantum mechanical amplitudes for interactions. Thus, GiBUU could be called a very sophisticated INC model. The passage of a hadron through the nuclear medium is then handled by a set of coupled integro-differential equations. Thus, required computer resources are significant.

GENIE, NEUT, and FLUKA have more standard INC models. They use free cross-sections for interactions but also apply medium corrections of various kinds. These corrections are less complete and more empirical than what is found in GiBUU. These models are most applicable for higher

energy hadrons (roughly pions with kinetic energy larger than 300 MeV and nucleons above 200 MeV), where the mean free path is long compared to the inter-nuclear spacing of roughly 1.8 fm and the pion Compton wavelength.

Peanut (FLUKA) [8] received a major effort 1995–99 and is very well adapted to describe processes from 10 MeV to 100 GeV. They include effects such as coherence time, refraction, and pre-equilibrium/compound nucleus processes which simulate known quantum mechanical features. NEUT FSI is based on the work of Salcedo, Oset, Vicente-Vacas, and Garcia-Recio [2]. This is a “ $\Delta$  dominance” model such as were common in the 1980’s when pion–nucleus physics was important in nuclear physics. It has the advantage of doing a careful job simulating the pion–nucleus interaction through  $\Delta(1232)$  intermediate states.

### 3. Systematics of hadron–nucleus data

Each nucleus has  $A$  nucleons =  $Z$  protons +  $N$  neutrons. All nuclei of interest to neutrino physics are either bound or slightly unbound. Nuclear densities show saturation because of short range repulsion. Therefore, the typical nucleus is approximately a sphere of radius proportional to  $A^{1/3}$ . The charge density of light nuclei ( $A < 20$ ) is found to be Gaussian or modified Gaussian. Heavier nuclei are described by the Woods–Saxon shape,

$$\rho(r) = N_0 \frac{1}{1 + e^{(r-c)/z}}, \quad (2)$$

where  $c$  describes the size and  $a$  describes the width of the surface of a nucleus. For example,  $c = 4.1$  fm and  $z = 0.55$  fm for  $^{56}\text{Fe}$ . To good accuracy,  $c$  is the radius where the density falls to half the central value with  $c \sim 1.2$  fm  $A^{1/3}$  and  $z \sim 0.55$  fm.

Hadrons interact with nuclei in a variety of ways. We use historical definitions of final states that come from interpretation of experiments. In *elastic scattering*, the final state nucleus is in its ground state and the hadron has same charge as the beam particle. If the hadron scatters inelastically, the residual nucleus can be the ground state or the nucleus can break apart. At low excitation energies ( $\lesssim 10$  MeV), the residual nucleus decays to a photon and the ground state. (This is important in analysis of SuperKamiokande data.) At higher excitation energies, one or more nucleons are emitted. Final state interactions increase this number. If there is a hadron of the same type but different charge in the final state, we call it *charge exchange*. For example, the reaction  $\pi^- p \rightarrow \pi^0 n$  is very common inside nuclei. As a boson, the pion can disappear inside the nucleus. Pion initiated reactions with no pions in the final state are called *absorption*. (This provides an important background process to neutrino quasielastic scattering.) For incident nucleons, most of these labels apply exactly. Since they cannot be absorbed, final

states with two or more nucleons are called *spallation*. If the hadron has enough energy, a pion (a second pion if the initial hadron is a pion) can be produced in the nucleus. We call those events *pion production*.

For low energy incident particles, these definitions are clean. At higher energies, the states mix and confusion can result. For example, a reaction  $\pi^+ {}^{12}\text{C} \rightarrow \pi^+ \pi^0 {}^{12}\text{C}$  can be inelastic, charge exchange, or pion production. Definitions we use call it pion production. A way to avoid difficulties is to measure inclusive cross-sections; there, the energy and angular distribution of a particular particle are determined. In each case, various reactions are possible but models can be tested without ambiguity.

Because the MFP is so short for hadron interactions, elastic scattering cross-sections look very diffractive. In fact, the angular distribution can be calculated with a quantum mechanical model using a black disk for the nucleus. This wave property is very difficult to simulate in a semi-classical or INC model.

Another consequence of the short MFP is seen in the total reaction cross-section ( $\sigma_{\text{reac}} = \sigma_{\text{tot}} - \sigma_{\text{elas}}$ ). For hadrons, this is close to the nuclear size,  $\pi R^2$ . For example,  $\sigma_{\text{reac}}$  for protons and neutrons of 0.4–1 GeV is flat at a value of about 300 mb = 30 fm<sup>2</sup> for carbon and about 80 fm<sup>2</sup> for iron. These corresponds to a radius,  $R$ , of about 3 and 5 fm. These values are close to the radius where the nuclear density is about half of the central value. If we divide these values by  $A^{1/3}$ , the result is close to the commonly used value of 1.2 fm. The pion–nucleus reaction cross-section at kinetic energies of about 85–315 MeV is dominated by the effect of the  $\Delta(1232)$  resonance. Thus, the effective size of the nucleus here is at a radius where the density is about 1% of the central density. For total cross-sections, the  $A$  dependence is often a power relation,  $\sigma \propto A^\alpha$ , but  $\alpha$  will vary from the expected value of 2/3 due to more complicated dynamics. The total cross-section for pion–nucleus has a power of about 0.8 for a wide range in energy. The  $A$  dependence of  $\alpha$  [14] varies between 0.55 and 0.8 for the components of the total reaction cross-section as a function of energy and process.

Nevertheless, many inelastic cross-sections have prominent contributions from *quasifree* interactions. Here, the hadrons in the final state have the kinematics as though they came from a single interaction between the incident particle and a nucleon in the nuclear medium. The name comes from the fact that nucleons in the nuclear medium are in a bound state and therefore not free. If the nucleon were free, the scattered particles would have a single energy at each angle. The struck nucleons have momentum (called Fermi motion), giving particles a range of momentum at a given angle. The largest momentum a nucleon can have is well-defined in the Fermi Gas model, is approximate in real nuclei. It is called the *Fermi momentum* and its value is approximately 250 MeV/ $c$ . In heavy nuclei, the average binding energy is

about 25 MeV. Thus, the peak due to quasifree scattering from a bound nucleon is shifted by about 40 MeV from the free case and the width is roughly 100 MeV.

This process has been widely studied for electron and pion probes. If it could be studied with neutrinos, the same structure would be seen. The so-called quasielastic peak is prominent in the inclusive scattering cross-section. At high excitation energies (lower kinetic energy for the scattered particle), a second peak is found for quasifree pion production from a bound nucleon. Final state interactions are more important in the details in this case. Consider the case of  $\pi^+$  interactions in carbon at 245 MeV. Evidence for quasifree pion scattering is strong. A scattered  $\pi^+$  is tagged on one side of the beam and the spectrum of protons is measured on the other side. A prominent peak is seen close to the angle where protons would be if the target was a free proton. The same correlation is seen between two protons where the  $\pi^+$  is absorbed on a quasideuteron in the nuclear medium. Strong evidence for quasifree pion scattering and absorption is seen. Calculations with an INC model are in excellent agreement with these data.

The energy distribution of  $\pi^+$  detected at  $130^\circ$  [3] shows a peak close to where scattering from a free proton would be seen. Since Fig. 2 (left) is for a  $\text{H}_2\text{O}$  target, scattering from H is seen as a gap at about 130 MeV (cross-section is too large to show). Pions interacting with oxygen nuclei produce a peak at about 100 MeV. Calculations show it is dominated by events with a single scattering (S). At low energies, the distribution is modified by events with more than one scattering (M). At forward angles, the contributions from multiple scattering are more important.

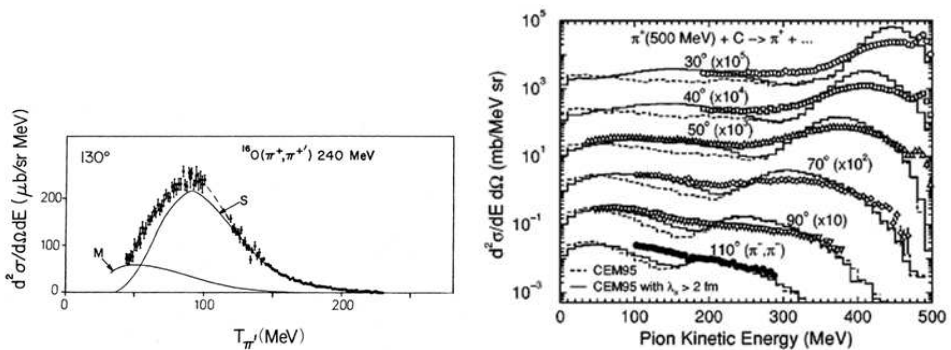


Fig. 2. Left: Inclusive  $\pi^+$  scattering data from Ingram *et al.* compared with separate curves for single and multiple scattering contributions. Beam energy is 240 MeV and target is water. Right: Inclusive  $\pi^-$  scattering data from Zumbro *et al.* compared with INC calculations of Mashnik *et al.*

If incident particles have a higher energy, complications can be found. With light targets, FSI effects are small and quasifree scattering and pion production peaks are seen. However, INC calculations have trouble getting the shape right, particularly in the region between the peaks. Fig. 2 (right) is for  $\pi^-$  scattering from  $^{12}\text{C}$  at 500 MeV [4]. For  $\pi^+$  absorption, the quasifree process would be  $\pi^+d \rightarrow pp$  since pions are highly unlikely to be absorbed on a single nucleon. LADS data [5] for  $\pi^+$  absorption in Ar ( $A = 40$ ) shows the largest strength for the  $pp$  final state but this is less than half of the total cross-section.

#### 4. INC models

Prominence of the quasifree reaction mechanism shows why INC models are valuable. These models assume the nucleus is an ensemble of nucleons which have Fermi motion and binding energy. The incident particle interacts in a series of encounters with single nucleons called a cascade (see Fig. 3).

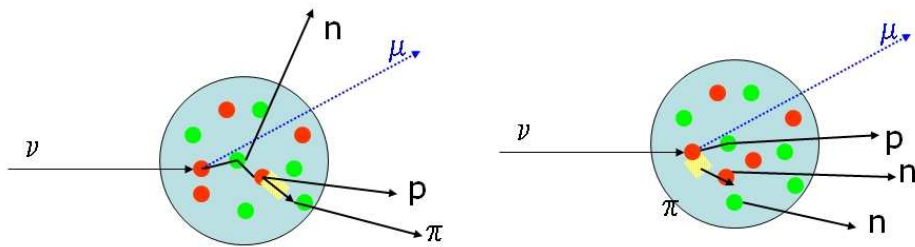


Fig. 3. Left: Schematic diagram for reaction involving typical FSI process. Right: Schematic diagram for reaction where pion is produced then absorbed in the same nucleus.

All interactions are governed by the cross-section for the free process, *e.g.*  $\pi^+n \rightarrow \pi^+n$  or  $pp \rightarrow pp$ . Probability of interaction is governed by a mean free path according to Eq. (1). Cross-sections for pions, kaons, protons, and photons interacting with free nucleons are fit with a partial wave analysis with results provided by the GWU group [13]. Nucleon densities come from compilations; note that neutron and protons have very similar densities even for nuclei such as lead.

The problems with INC models must be considered. Since interactions are governed by cross-sections rather than quantum mechanical amplitudes, the nuclear model is often very simple. The simplest and most general nuclear model is the Fermi gas which is the basis for all neutrino–nucleus event generator models. Effects of nucleon correlations (see talk in this school by Benhar) must be included empirically. Both the struck nucleon

and the scattered hadron are likely to be off-shell. Although this effect has been shown to be “moderate”, it is difficult to simulate in a semi-classical model. Thus, there is no definite prescription for an INC model; many versions exist with a wide range of applicability.

The successes of INC models are large. For many reactions, they are the only models available for comparison. They were first used for pion production in proton–nucleus interactions by Metropolis and Harp [10]. A general INC model (CEM03) developed by Mashnik and collaborators [11] has been applied with success to a wide range of pion– and proton–nucleus data [12]. Examples are shown in Figs 4 and 2 (right); we will show similar comparisons for the GENIE FSI model.

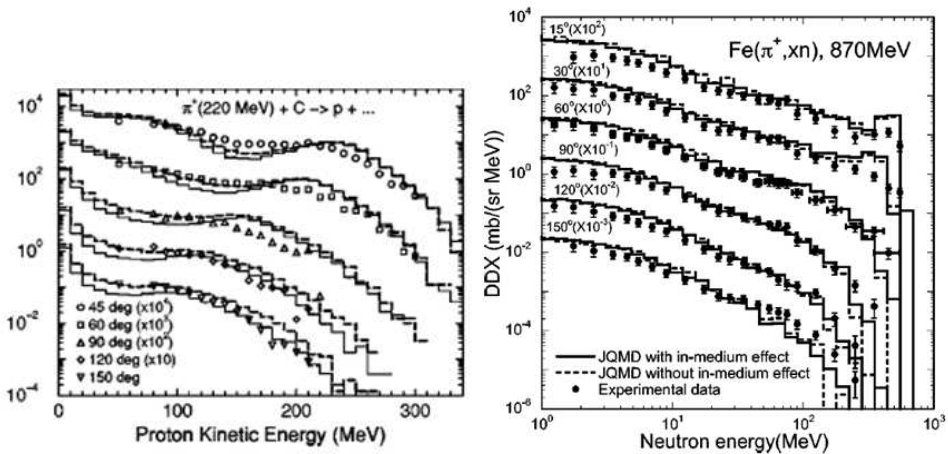


Fig. 4. Left: Mashnik *et al.* INC calculations compared with McKeown *et al.* data. Right: Mashnik *et al.* INC calculations compared with Iwamoto *et al.* data.

The FSI model in FLUKA is PEANUT; it is described in this school by Battistoni. This uses a more sophisticated INC model than CEM03. Various nuclear and quantum mechanical corrections are applied. The result is impressive agreement with a wide variety of data.

Treatment of pion absorption is somewhat different in the INC models than the  $\Delta$  dominance models. In the latter, pions first rescatter off a nucleon (off-shell) and then absorbed on another. There are other mechanisms which should be included. Salcedo, Oset, Vicente-Vacas, and Garcia-Recio [2] include both  $S$ -wave absorption and 3-body absorption. In INC, the fundamental process for pion absorption is  $\pi^+ d \rightarrow pp$  and this is often the only process included. Since the density of nucleons is much smaller in deuterium as compared with real nuclei, an empirical factor (with a value often about 3) must be included.



## 5. FSI models in GENIE — hA

GENIE [1] is a universal neutrino–nucleus event generator that can be applied to all experiments for 0.1–100 GeV neutrinos. It is already the event generator for most experiments that are running or planned. It has models for all types of neutrino interactions. It is based on a Fermi gas model of the nucleus. This can be readily applied to every nucleus with qualitative accuracy.

The first FSI model [17] is in the spirit of the other models in GENIE. It is simple and empirical, data-driven. Rather than calculate a cascade of hadronic interactions as is done in a complete INC model, we use the total cross-section for each possible nuclear process for pions and nucleons as a function of energy up to 1.2 GeV. Thus, it is called hA. The emphasis is on iron because the first application was to MINOS where production of high energy pions is important. At low energies (50–300 MeV), there is sufficient data [14–16] for a good description. At high energies, only a few data points are available. Here, we use results obtained for the CEM03 model. Although the calculations are complete, they are not in good agreement with the existing total cross-section data. Therefore, the calculations are normalized to the data at low energies. Elastic data at high energy are used to extrapolate the model to 1.2 GeV.

The hA model also handles proton and neutron rescattering. The same reactions are possible except that neither can be absorbed. Still, multinucleon knockout is highly probable. Although much less data is available for nucleons than pions, CEM03 was tuned primarily for them.

The values used for  $\pi^+$  and  $p$  are shown in Fig. 5. Data values are used for energies below 315 MeV for all cross-sections. Total cross-section data is available across the entire range. Data for total and total reaction cross-sections are used across the entire range in energy. Cross-sections for targets other than iron are obtained by scaling by  $A^{2/3}$ . As discussed above, this is a reasonable approximation. Because such a large range is covered, processes such as pion production must be included. Here, we use the CEM03 calculations.

The total cross-section is calculated from the mean free path and can be checked against data. In addition the accuracy of the  $A^{2/3}$  scaling can be checked with data from another target. We show the component total cross-sections for the model compared with carbon data in Fig. 6. (Agreement for iron has less information and is equal in quality.)

All the data points in Fig. 5 have error bars. These are either taken from the data or estimated. These provide the range of values sampled during reweighting exercises. This is an excellent way to estimate model dependent errors in a neutrino oscillation experiment (see the contribution from Jim Dobson to this workshop). The ability to reweight is an important feature of this model.

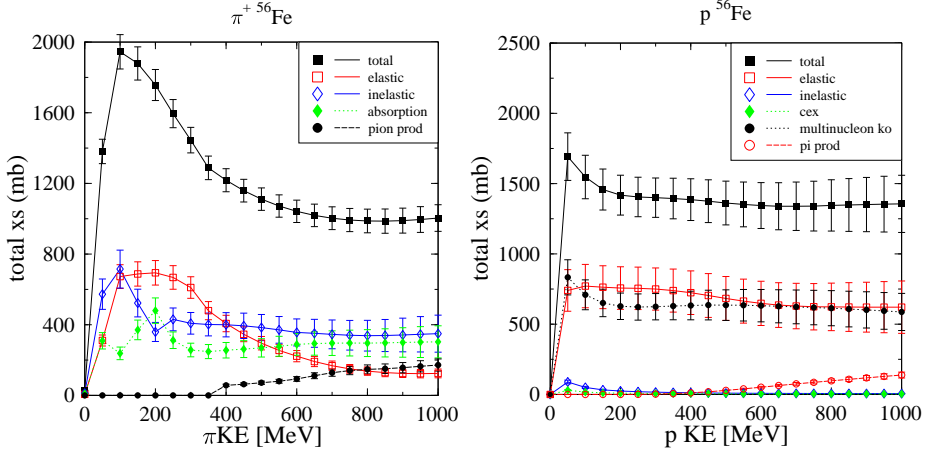


Fig. 5. Left: Total cross-sections for  $\pi^+$  Fe reactions used in GENIE hA model. Final states are chosen according to these values. Right: Same for  $p$  Fe reactions.

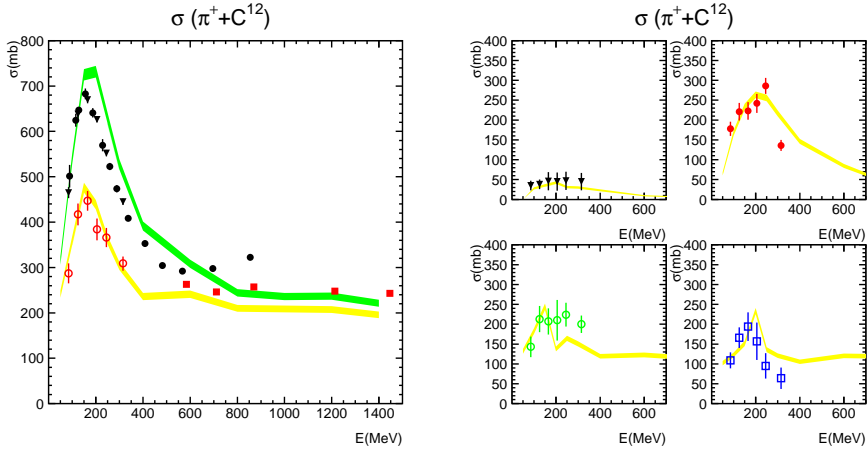


Fig. 6. Left: Total cross-sections for  $\pi^+$  C reactions. GENIE hA model is used. Total cross-section is determined with proper mean free path in a carbon nucleus. Right: Component cross-sections come from the corresponding iron cross-sections scaled by  $A^{2/3}$ .

This is the default FSI model in GENIE version 2.4.0, the public version as of now. It uses identical cross-section for  $\pi^+$  and  $\pi^-$  and for  $p$  and  $n$ . For isoscalar targets, *e.g.*  $^{12}\text{C}$  and  $^{16}\text{O}$ , this is no issue for the pions because of isospin symmetry. For targets such as lead, this is a 10% effect. The charges of particles in the final state tend to reflect the charge of the probe. For example, final states for  $\pi^+$  have more protons than neutrons while the

opposite holds for  $\pi^-$ . Cross-sections for  $\pi^0$  beams cannot be measured. This code uses isospin symmetry to calculate them from the charged pions. The total reaction cross-sections for  $p$  and  $n$  are very similar, plots are shown in the next section. Charges of final state particles tend to be more positive for incident protons.

Pion absorption and nucleon spallation reactions can knock out large numbers of nucleons. This is seen strongly in data. More detailed calculations (see below) show an average of 10 nucleons ejected from iron in pion absorption. To simplify the code, the hA model limits this to 5. For MINOS, this is never an issue.

Angular and energy distributions of particles are estimated. For elastic scattering, template angular distributions from relevant data are used. These distributions are very forward peaked, so it is not an important simplification. For final states with more than 1 hadron, particles are distributed by phase space. This gives the correct limits, but the energy distribution changes somewhat when the  $\Delta$  resonance dominates. The effect of these approximations have not yet been simulated, but they are unlikely to be an important effect in the MINOS experiment. One of the most significant errors is in the treatment of the quasielastic scattering. Only the incident particle is put in the final state and its energy and angle distribution are both flat.

Since the elastic cross-section cannot be generated in an INC model, it has to be added on. For the hA model, we chose an empirical method. The size of the nucleus is increased by  $\Delta R$  which is proportional to the de Broglie wavelength. This nicely matches the data for all energies.

Almost all of the problems in the last paragraphs will be fixed in **GENIE** version 2.6.0. Changes due to isospin in either hadron or nucleus will be greatly improved. The number of final states sampled will be increased. Inelastic final states will be assumed to be dominated by quasielastic events. (This approximation can be checked against data and will be discussed in the next section.)

## 6. FSI models in GENIE — hN

The second FSI model in **GENIE** (hN) is a full INC model. It includes interactions of pions, nucleons, kaons, and photons in all nuclei. The basis is the angular distributions as a function of energy for about 14 reactions from threshold to 1.2 GeV. All this information comes from the GWU group [13] A preliminary version of the hN model is scheduled to be in **GENIE** v. 2.6.0, but the hA model will still be the default.

As a full INC model, all reactions on all nuclei can be calculated. None of the restrictions that apply to hA model are relevant. Although the choice of interaction points through the MFP is identical in the two models, the cascade is fully modeled in the hN model. For example, there is a small but finite probability of knocking out every nucleon in an event.

One new feature of this code is the inclusion of nucleon pre-equilibrium and compound nuclear processes. The present model is simple, but effective. This is important to give an improved description of the vertex energy deposition.

The code was designed to minimize the number of parameters. One parameter scales the absorption MFP and is fit to the pion total absorption cross-section. Separate values for the  $\Delta R$  values for pions and nucleons are fit to the total reaction cross-sections. All particles get a free step when they are produced; this simulates the effect of  $\Delta$  resonance propagation in a simple way. It is used to adjust the normalization of certain inclusive scattering distributions. A shift in the energy of nucleons in the nucleus is used to put the quasielastic peak (see Fig. 2 (left)) (similar to what is used in electron scattering).

The validation of this new code comes in two parts — the total cross-sections for various processes (*e.g.* Fig. 6) which test the overall propagation of particles and the inclusive cross-sections [*e.g.* Figs 2 (right) and 4]. Each is important. Previous validations emphasize the total cross-sections because this sets the overall flow of particles into each topology. Previous neutrino experiments emphasize topology. Future experiments are expected to put emphasis into the distribution of particles in energy and angle as beam and detector technology improve.

The component total cross-section data is limited to hadron energy of less than  $\sim 350$  MeV. The exception is the total reaction cross-section which has been measured for  $\pi^+$ ,  $\pi^-$ ,  $p$ , and  $n$  up to roughly 1 GeV. Figure 7 shows  $\sigma_{\text{reac}}$  for protons in iron and neutrons in carbon. The energy dependence is flat and we see the cross-section approximately equal to the nuclear area as discussed in the introduction. Agreement of the model is excellent.

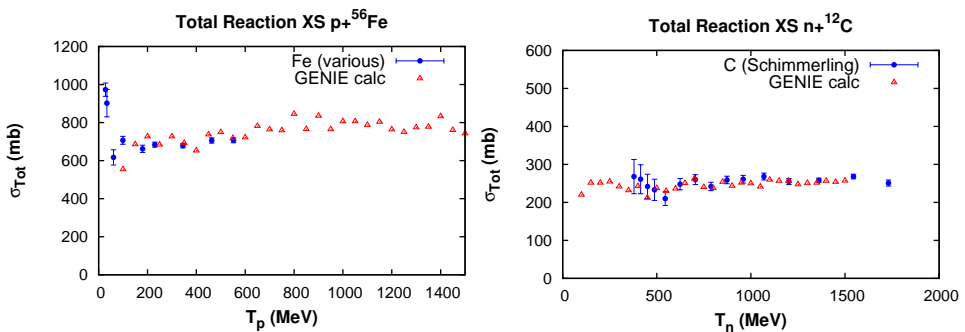


Fig. 7. Left: Total reaction cross-sections for  $p$  Fe reactions from the GENIE hN model. Right: Total reaction cross-sections for  $n$  C reactions from the GENIE hN model.

For pions, comparisons with the hA model are shown above. Now, the cross-sections are calculated microscopically. In Fig. 8, we show  $\sigma_{\text{reac}}$  for pions. The agreement is excellent except at low energies for heavier targets; this is still under study. With the significant interest in absorption, we show two examples of that total cross-section in Fig. 9. Overall agreement is very good, but the problem in  $\sigma_{\text{reac}}$  at low energies for heavy targets is shown to be in the absorption channel. Continuing with absorption, we show two examples similar to Fig. 4 in Fig. 10. The agreement shown here is excellent as the details of pion reactions are explored across a wide kinematic range.

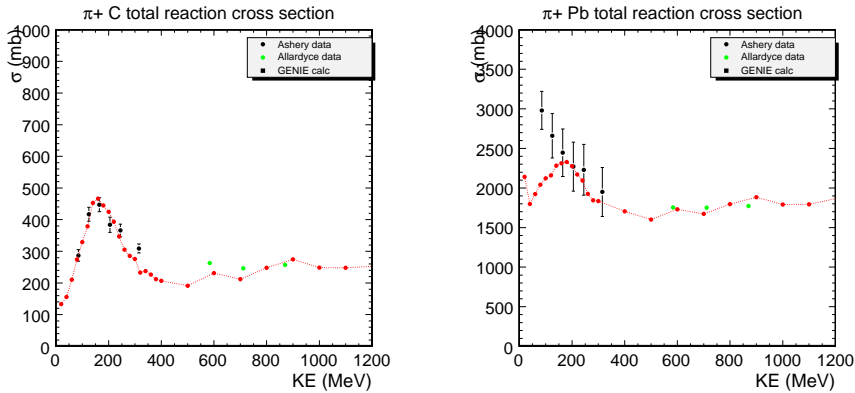


Fig. 8. Left: Total reaction cross-sections for  $\pi^+$  C using the GENIE hN model compared to data. Right: Total reaction cross-sections for  $\pi^+$  Pb using the GENIE hN model.

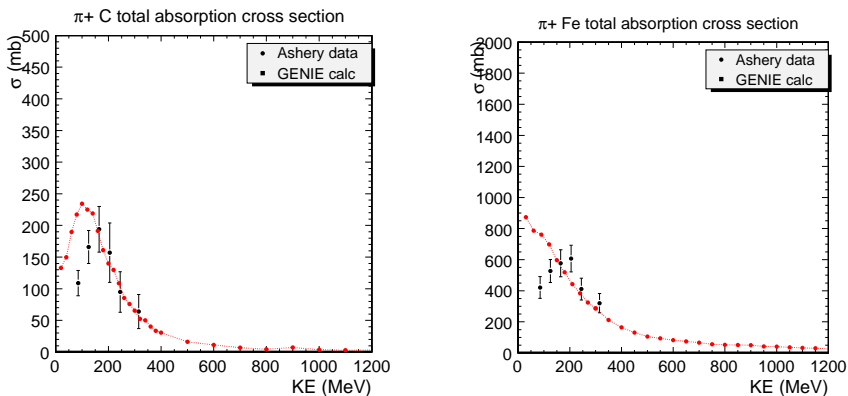


Fig. 9. Left: Total absorption cross-sections for  $\pi^+$  C using the GENIE hN model compared to data. Right: Total reaction cross-sections for  $\pi^+$  Pb using the GENIE hN model.

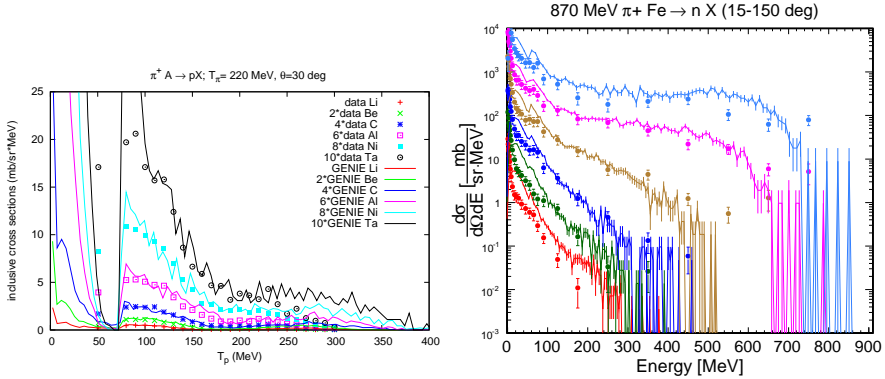


Fig. 10. Left: Inclusive cross-sections for protons emitted from 220 MeV  $\pi^+$  interacting in various nuclei. In each distribution, protons are detected at  $30^\circ$ . Data is from McKeown *et al.* These protons come from both absorption and scattering processes. Right: Inclusive cross-sections for neutrons emitted from 870 MeV  $\pi^+$  interacting in iron. In each case, neutrons are detected at different angles. Data is from Iwamoto *et al.* These neutrons come from predominantly the absorption process.

The last example of this new code is for scattering processes. When hadrons interact in the nuclear medium, the quasifree scattering process is important; that has been seen in numerous data sets. In Fig. 11, we show examples for pion and proton scattering. For the pion case, a back angle is shown; here, the quasielastic mechanism dominates. For protons, the beam energy is large enough that the multiple scattering process is sampled over a wide range in energy. The agreement is excellent.

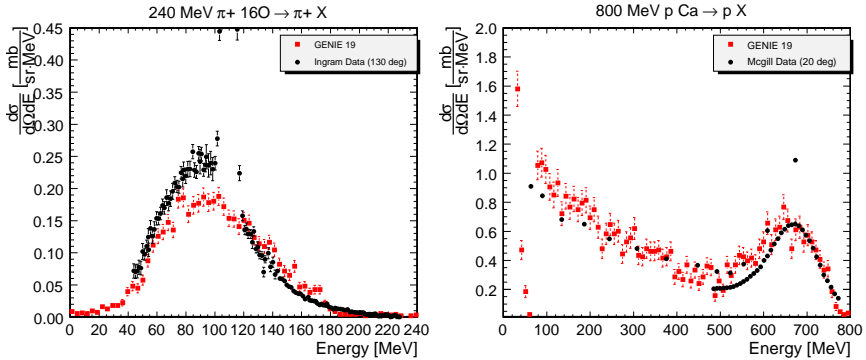


Fig. 11. Left: Inclusive cross-sections for  $\pi^+$  scattered at  $130^\circ$  from 240 MeV  $\pi^+$  interacting with oxygen. At this back angle, the spectrum of  $\pi^+$  is dominated by the quasifree mechanism. Data is from Ingram *et al.* Right: Inclusive cross-sections for protons scattered at  $20^\circ$  from 800 MeV protons interacting with calcium. Data is from McGill *et al.* and Chrien *et al.* There is a known absolute normalization difference between the two experiments but it is not available to us.

## 7. Conclusions

We have reviewed strong interactions as they will be applied to neutrino experiments of the near future. The basic premise is that hadron–nucleus experiments are the best way (definitely now, likely also in the future) to validate FSI models. General properties have been identified from data, the general blackness of nuclei to hadrons along with the importance of quasifree mechanisms.

Various models were discussed with a focus on INC models. Although, they are not the most theoretically viable, the role of INC models is significant because they can “easily” describe a wide range of data.

The two FSI models in **GENIE** are described in some detail. The hA model is simpler and more empirical. Although it is not the most accurate, it is very fast and straightforward to reweight. The hN model is a full INC calculation which is much more accurate. In version 2.4, the hA model is the only FSI model. For version 2.6, both will be included but hA will still be the default. The hA model will be applicable to all nuclei from helium to lead for kinetic energies up to 1.2 GeV for pions and nucleons. Its main value will be for high energy neutrinos and in reweighting. The hN model is nearly complete for this round. It will be valid for energies above 50 MeV and will provide a very complete description of many final states.

Thus, each **GENIE** FSI model has independent validity. An important component of any simulation is the estimation of systematic errors. A comparison of the results using each model can show model dependence. Varying parameters inside the hA model is the best way to assess systematic errors due to FSI.

## REFERENCES

- [1] C. Andreopoulos *et al.* [arXiv:0905.2517 \[hep-ph\]](#), submitted to *Nucl. Instrum. Methods*.
- [2] L.L. Salcedo, E. Oset, M. Vicente-Vacas, C. Garcia-Recio, *Nucl. Phys.* **A484**, 557 (1988).
- [3] C.Q.H. Ingram *et al.*, *Phys. Rev.* **C27**, 1578 (1983).
- [4] J. Zumbro *et al.*, *Phys. Rev. Lett.* **71**, 1796 (1993).
- [5] B. Kotlinski *et al.*, *Eur. Phys. J.* **A9**, 537 (2000).
- [6] T. Leitner, L. Alvarez-Ruso, U. Mosel, *Phys. Rev.* **C73**, 065502 (2006).
- [7] A. Engel, W. Cassing, U. Mosel, M. Schäfer, Gy. Wolf, *Nucl. Phys.* **A572**, 657 (1994); O. Buss, T. Leitner, U. Mosel, L. Alvarez-Ruso, *Phys. Rev.* **C76**, 035502 (2007).
- [8] A. Ferrari, P.R. Sala, Proc. of the Int. Conf. on Nuclear Data for Science and Technology (NDST-97).

- [9] R. Merenyi *et al.*, *Phys. Rev.* **D45**, 743 (1981); W.A. Mann, private communication.
- [10] G.D. Harp, *Phys. Rev.* **C10**, 2387 (1974).
- [11] S.G. Mashnik, K.K. Gudima, A.J. Sierk, M.I. Baznat, N.V. Mokhov, LANL Report LA-UR-05-7321 (2005), RSICC Code Package PSR-532; S.G. Mashnik, A.J. Sierk, K.K. Gudima, M.I. Baznat, *J. Phys.: Conference Series* **41**, 340 (2006) [[nuc1-th/0510070](#)]; S. Mashnik, private communication.
- [12] S.G. Mashnik, R.J. Peterson, A.J. Sierk, M.R. Braunstein, *Phys. Rev.* **C61**, 034601 (2001).
- [13] R.A. Arndt, W.J. Briscoe, I.I. Strakovsky, R.L. Workman, M.M. Pavan, *Phys. Rev.* **C65**, 025213 (1994); <http://gwdac.phys.gwu.edu>
- [14] D. Ashery *et al.*, *Phys. Rev.* **C23**, 2173 (1981); I. Navon *et al.*, *Phys. Rev.* **C28**, 2548 (1983).
- [15] A.S. Carroll *et al.*, *Phys. Rev.* **C14**, 635 (1976); A.S. Clough *et al.*, *Nucl. Phys.* **B76**, 15 (1974).
- [16] W. Bauhoff, *At. Data Nucl. Data Tables* **35**, 429 (1986).
- [17] S. Dytman, H. Gallagher, GENIE-PUB/2007/003.3; <http://pub.genie-mc.org>